Pramana – J. Phys., Vol. 38, No. 6, June 1992, pp. 641–667. © Printed in India.

Magnetization studies in niobium and $YBa_2Cu_3O_7$ samples

B V B SARKISSIAN[a,c], A K GROVER[a,d], G BALAKRISHNAN[a,e], RAVI KUMAR[a], P L PAULOSE[a], R VIJAYARAGHAVAN[a], V SANKARANARAYANAN[b] and C K SUBRAMANIAN[b]

[a]Tata Institute of Fundamental Research, Homi Bhabha Road, Bombay 400005, India
[b]Department of Physics, Indian Institute of Technology, Madras 600036, India
[c]Present Address: Centro Brasileiro de Pesquisas Fisicas -CBPF/CNP$_q$, Rua Dr. Xavier Sigraud 150, 22290 Rio de Janeiro, Brazil
[d]Present Address: Department of Physics, Panjab University, Chandigarh 160014, India
[e]Present Address: Department of Physics, University of Warwick, Coventry CV4 7AL, UK

MS received 2 November 1991; revised 17 March 1992

Abstract. The results of experimental studies on hysteresis in magnetization, thermomagnetic history effects, anomalous variations in magnetic hysteresis curves and the decay rates of magnetization obtained under different thermomagnetic histories in specimens of conventional and high temperature superconductors are presented. The Bean's critical state model is considered adequate to explain magnetic behaviour in conventional hard superconductors. The similarity in the general features of the results of different experiments on specimens of the two families of superconductors underscores the efficacy of the said model to understand some aspects of the macroscopic magnetic response of high temperature superconductors as well. For instance, the isothermal magnetization hysteresis loop which comprises of magnetization curves along forward ($-H_{max}$ to $+H_{max}$) and reverse ($+H_{max}$ to $-H_{max}$) paths define an envelop within which all isothermal magnetization data along different thermomagnetic histories lie. There exist inequality relationship between various field values identified as H_{peak}, H_I, H_{II} etc. in isothermal magnetization hysteresis as well as magnetic relaxation data. The entire field span of an isothermal magnetization hysteresis data set can be considered to comprise of three parts corresponding to $(M_{rem}(H) - M_{FC}(H) + M_{ZFC}(H))$ being equal to, less than or greater than zero, where $M_{rem}(H)$ are the remanent magnetization values obtained on reducing field to zero after having the specimen in different applied field (H) values. There are, however some situations amongst thermomagnetic history effects in specimens which show incomplete flux trapping on field cooling, where the critical state model has been found inadequate.

Keywords. Magnetization curves; critical current; Bean's model; anomalous magnetic behaviour; time dependence of magnetization.

PACS Nos 74·30; 74·60

1. Introduction

Magnetic hysteresis measurements play an important role in providing information about field and temperature dependence of critical current density, $J_c(H, T)$, in hard type II superconductors. This information *per se* is model dependent. The hysteresis observed in isothermal magnetization of hard superconductors was first related to J_c by C P Bean (1962, 1964). The advent of high temperature superconductors injected a renewed interest in expounding the physical basis of the critical state model due to Bean (1962, 1964). This interest has recently (Bhagwat and Chaddah 1989) led to raising the status of critical state model to the level of phenomenology such that

it emerges as the logical extension of the application of Lenz's law to hard superconductors. However, a few important issues related to the usage of this model in extraction of $J_c(H)$ from the magnetization data, in particular in high temperature cuprate superconductors, still need to be resolved. First, the theoretical calculations in the framework of Bean's model for various forms of $J_c(H)$ are generally available only for sample shapes that are infinitely long along the field direction and thus have demagnetization factor $N = 0$, whereas the experimental samples are of finite size ($N \neq 0$). One may argue that $N = 0$ approximations are relevant in experimental situations where the sample dimension D perpendicular to the field is infinitesimally small, however, it has been pointed out by Bhagwat and Chaddah (1990) that this technique would not suffice because the magnetic hysteresis decreases to zero as $D \to 0$. Another difficulty which emerges from recent theoretical work of Bhagwat and Chaddah (1989, 1991) on few finite shapes is that the Taylor series expansion of Feitz and Webb (1969) (used at field values larger than the limiting value of the applied field when the flux has fully penetrated the semi-infinite sample) which results in a linear relationship between the width of magnetic hysteresis ($\Delta M(H)$) and current density $J_c(H)$ cannot be used in finite-sized specimens in similar field region. A priori, the linear relationship between $J_c(H)$ and $\Delta M(H)$ may therefore not be valid in any field region in finite-sized specimens. However, it is hoped that few other general topological features pertaining to the isothermal magnetization curves which have been highlighted by Chaddah and coworkers (Chaddah *et al* 1989a, b; Chaddah and Ravi Kumar 1989c) and Chen and coworkers (Chen and Goldfarb 1989; Chen *et al* 1990a, b) on the basis of their analytical results in infinite geometries would be evident in the magnetization data on finite-sized specimens. To briefly recapitulate, these topological features relate to the existence of certain characteristic fields, like, H_{peak}, H_I, H_{II} etc. (these shall be defined at appropriate places in §§ 3 to 5), the inequality relationship amongst them, the shapes of the curves describing the field dependence of time decay rates of magnetization obtained along different paths, etc.. Lastly, the nature of the cuprate variety of high temperature superconductors is such that the coherence length normal to the planes of easier flow of J_c is much smaller than the spacing between neighboring Cu–O planes. These materials are therefore being modelled (Deutscher and Müller 1987; Malozemoff 1989; Malozemoff *et al* 1989 and Martin *et al* 1989) as stacks of 2D Cu–O superconducting sheets weakly coupled to each other via some kind of Josephson tunneling. This characteristic, some people argue (Malozemoff 1989), bestows on them a behaviour analogous to that expected in superconducting glasses and the experimental support for it is believed to come from certain archetypal characteristics in the thermomagnetic history and temporal effects in the magnetization data of these materials. In view of such approaches, it is of interest to carry out a comparison of the topological features seen in isothermal magnetization curves obtained under various thermomagnetic histories over differing ranges of H and T values in specimens of high temperature superconductors with those of conventional low temperature hard superconductors for which Bean's formalism is considered to be generally appropriate. We present here the detailed results of one such comparative study (a few highlights of this work have been reported earlier (Sarkissian *et al* 1989)) on a powder specimen of $YBa_2Cu_3O_7$ with two specimens of elemental niobium (an example of conventional low temperature

superconductors). The broad agreement between the behaviour observed in these two classes of materials underscores the general applicability of the critical state model to extract information on $J_c(H, T)$ and to understand the characteristics of thermo-magnetic history effects in high temperature superconductors.

2. Experimental

2.1 *Samples*

The powder specimens of $YBa_2Cu_3O_7$ used for different magnetization measurements were obtained by crushing down a part of the sintered pellet just before loading the specimen into a magnetometer. The niobium specimens used were in the form of (i) fine powder (purity 99·9% and sieved through 65 μ mesh) obtained from Koch-light, UK and (ii) a cylindrical piece ($l = 5$ mm, $\phi = 1{\cdot}3$ mm) machined out of a 6 mm diameter rod (purity 99·9%) obtained from Leico Industries, USA. The niobium specimens were not subjected to any outgassing procedure above ambient temperature. Niobium behaves as a hard type II superconductor because of absorbed oxygen and nitrogen (DeSorbo 1963, 1964; Finnemore *et al* 1966) and the extent of non-equilibrium behaviour in it is known to vary with heat treatment (DeSorbo 1963, 1964).

2.2 *Magnetization measurements*

The magnetization hysteresis curves were obtained using an Oxford instruments susceptometer based on the Faraday method and a quantum design MPMS SQUID magnetometer. For the Faraday method, the steady field (up to 80 kOe) and the gradient field were both produced by coaxial superconducting coils. The process of recording the force value was initiated a few minutes after attaining the steady field (overshoots and undershoots in field were avoided), which was continuously monitored. As far as possible, the sample was carefully located at the centre of the gradient coil assembly and the reversal of the field gradient was not resorted to while recording the force. The field gradient was switched-on and off once before being kept-on to record the force. The field gradient was limited to values less than 22 Oe/cm in most of the runs.

The powder specimens were put inside a cylindrical copper bucket having I.D. $\simeq 5$ mm and they filled the bucket up to a height of $\leqslant 4$ mm. Thus the spread in steady field distribution caused by the field gradient over the entire length of the sample never exceeded 10 Oe.

The isothermal magnetization measurements on different samples were made with the following histories:

1. *Complete hysteresis loop*: To record the complete hysteresis, the specimen was cooled down from above T_c to a given temperature in the residual field of the superconducting magnet (nominal zero field cooling (ZFC)) and the record of the compete hysteresis loop was made by ramping the field up to a chosen maximum field H_{max}, then reversing it to $-H_{max}$ (reverse hysteresis path) and finally reversing again to reach $+H_{max}$.

2. *Variation of remanent magnetization with* H_{max}: To ascertain this variation the specimen was cooled down from above T_c to a given temperature in nominal zero field. The field was then ramped up to a chosen maximum (H_{max}) followed by ramping it down to zero value. The remanent magnetization corresponding to a chosen H_{max} is then noted down. This process was repeated for different chosen H_{max} values.

3. *Thermomagnetic history effects after cooling in different field values*: The specimen was cooled down from above T_c to a given temperature in a given field (field cooling (FC)). The field was ramped up either to a certain maximum value or ramped down to zero value and taken towards $-H_{max}$ value. These data are needed to study the characteristics of thermomagnetic history effects.

The experimental results on isothermal magnetization curves are summarized in §§ 3 and 4.

3. Results

3.1 *Complete hysteresis loops*

Figures 1 and 2 show the magnetization hysteresis data recorded at 4·2 K in powder specimens of niobium and $YBa_2Cu_3O_7$ respectively. The data on niobium were recorded by Faraday method whereas those in $YBa_2Cu_3O_7$ were obtained on a

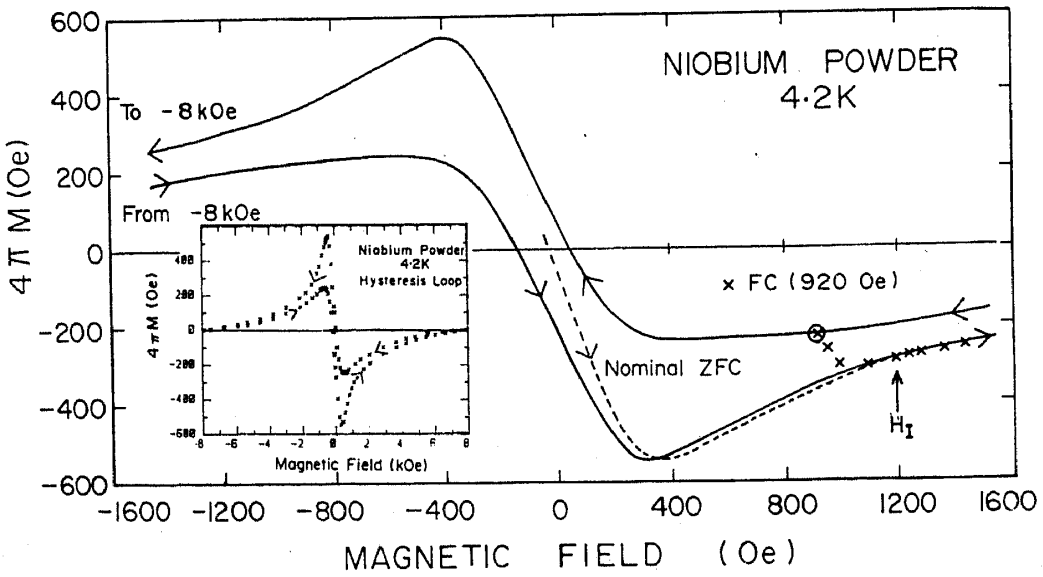

Figure 1. Magnetization hysteresis curve in a specimen of niobium powder at 4·2 K. The inset shows the complete hysteresis loop whereas the main figure shows the details in the central portion of the loop on an expanded scale. The sample was cooled down to 4·2 K in the residual field of the superconducting magnet (designated as nominal zero field) before ramping the field up. The arrows indicate the way the field was varied. The data were recorded at discrete field values, the continuous lines drawn are smooth curves through the closely spaced data points. The merger point of the nominal ZFC and forward hysteresis curve identifies $H_I(\simeq 1200\,\text{Oe})$ value for niobium powder at 4·2 K. The encircled cross data point denotes the measured magnetization value on cooling the sample from above 10 K down to 4·2 K in a field of 920 Oe. The crossed data points show the magnetization values as the field was increased upwards from 920 Oe after field cooling.

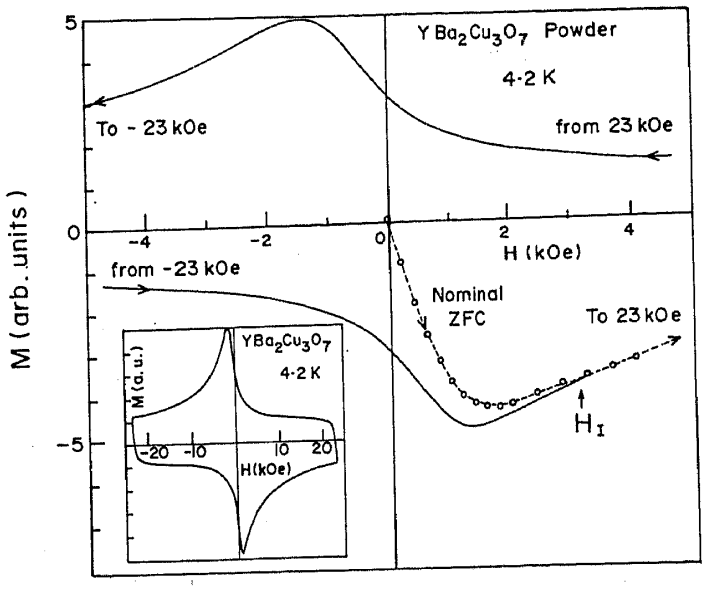

Figure 2. The magnetization hysteresis curve in a powder specimen of $YBa_2Cu_3O_7$ at 4·2 K. The inset shows the complete hysteresis loop obtained in a field of ± 23 kOe. The main figure shows the details in the central portion of the loop on an expanded scale. The sample was cooled down to 4·2 K in nominal zero field before cycling the field in the forward and reverse directions. The merger point of the nominal ZFC and forward hysteresis curves identifies the $H_I(\simeq 3\,\text{kOe})$ value in this specimen at 4·2 K.

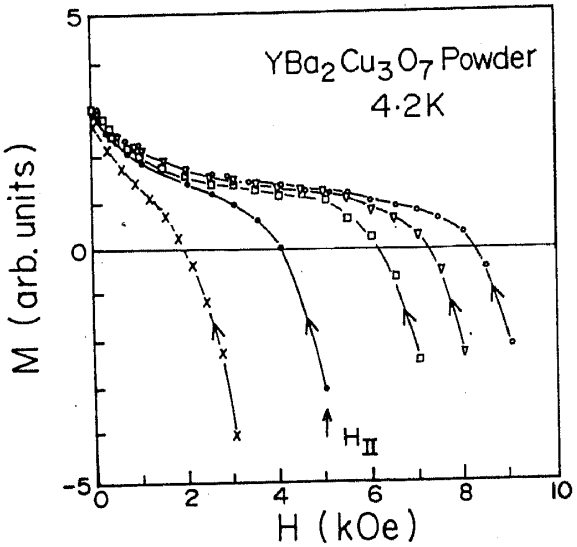

Figure 3. Magnetization curves in $YBa_2Cu_3O_7$ powder sample on reversal of field from chosen maximum (H_{max}) values. For each of these curves, the sample was first cooled down to 4·2 K in nominal zero field and the field was then ramped up to a chosen H_{max} value. The magnetization data were recorded at discrete field values on reversal of field down to zero value, from a given H_{max} value. $H_{II}(O)$ identifies the limiting field H_{max} value, reversal from which remanence magnetization reaches the saturation value for this specimen at 4·2 K.

SQUID magnetometer. As stated earlier the magnetization data were recorded at discrete field values, most of the continuous plots depicted in figures 1 and 2 are smooth curves drawn through the data points. Figure 3 shows the magnetization curves at 4·2 K in $YBa_2Cu_3O_7$ recorded on reversal of magnetic field from different H_{max} values.

Figures 1 and 2 depict the details of the nominal ZFC, reverse hysteresis (from $+H_{max}$ to $-H_{max}$) and forward hysteresis (from $-H_{max}$ to $+H_{max}$) curves. The insets in figures 1 and 2 show the complete hysteresis loops that are obtained on repeated cycling the field between $\pm H_{max}$. An important qualitative difference between the hysteresis curves shown in the insets of figures 1 and 2 is that the curve in Nb powder (figure 1) is mainly contained in the second and fourth quadrant whereas that for $YBa_2Cu_3O_7$ (figure 2) spans all the four quadrants. The former type of response indicates partial reversibility (i.e., spontaneous escape of some magnetic flux such that the equilibrium magnetization contributes significantly to the total magnetization being measured), whereas the latter implies near complete irreversibility. The calculated magnetization curves based on Bean's critical state model (Chaddah *et al* 1989a, b; Chaddah and Ravi Kumar 1989c; Chen and Goldfarb 1989; Chen *et al* 1990a, b) include effects only due to infinite conductivity of the sample, the contribution of the equilibrium magnetization of the specimen is usually considered to be insignificant. A characteristic fact which distinguishes between the equilibrium magnetization curve and the calculated magnetization curve obtained via critical state model is the sign of the differential magnetization (dM/dH) on reversal from a $H_{max}(> H_{peak}$, where H_{peak} is the field value at which ZFC magnetization curve peaks). A magnetization hysteresis curve which is dominated by a contribution from equilibrium magnetization would have dM/dH as positive whereas in the case of critical state model dM/dH is negative in the said region. The calculated curves may sometimes be viewed as being of limited relevance for specimens where equilibrium magnetization is a significant part of total magnetization. However, there is a topological feature which is common to the curves in figures 1 and 2. There exists a characteristic field value at which the virgin (nominal ZFC) magnetization merges with the forward hysteresis curve, above this field the magnetization curve is independent of the previous history of the applied field. In analogy with an argument (Chaddah *et al* 1989b; Chaddah and Ravi Kumar 1989c) put forward on the basis of calculations for semi-infinite geometries, this field value may be identified with the limiting value of applied field (designated as H_I) at which the flux penetrates the entire volume of a finite sized specimen. H_I values in the given powder specimens of Nb and $YBa_2Cu_3O_7$ at 4·2 K are 1·2 kOe and 3 kOe respectively. H_I values in any specimen, in general, depends on the Bean's (Bean 1962) parametric field H^* ($\propto J_c(0) \times$ dimension of sample perpendicular to the field) and the functional form of $J_c(H)$. For infinite slab and cylindrical shaped specimens, Chaddah *et al* (1989b) have given explicit expression for a few simple forms of $J_c(H)$. From these, it is apparent that, in general, $H_I \geqslant H^* \geqslant H_{peak}$. The equality relationships holds only for infinite samples when $J_c(H) = \text{constant}$. For $J_c(H)$ decaying very rapidly with H, it is expected that $H_{peak} \ll H^*$. Though H^* increases linearly with sample size, the H_I does not. In general, the dependence of H_I on sample size is considerably less than linear.

It has also been stated (Chaddah *et al* 1989b; Chaddah and Ravi Kumar 1989c) that H_I values satisfy the inequality, $2H_I > H_{II}(H_{max})$, where $(H_{max} - H_{II}(H_{max}))$ is the field interval below the maximum field H_{max} (to which the sample was exposed before reversal) where the Taylor series expansion of Fietz and Webb (1969) is not valid. $H_{II}(H_{max})$ decreases as H_{max} increases, the limiting value of $H_{II}(H_{max})$ is denoted by $H_{II}(0)$, (Grover and Chaddah 1991) such that $2H_I \geqslant H_{II}(0) \geqslant H_{II}(H_{max})$. $H_{II}(0)$ is argued (Chaddah *et al* 1989b) to equal the field value, reversal from where causes the remanence magnetization to reach its saturation value. Figure 3 shows that in the

given $YBa_2Cu_3O_7$ powder sample the remanance reaches its saturation value on reversal from $H_{max} \geqslant 5$ kOe. If we identify this limiting value to be $H_{II}(0)$ for this $YBa_2Cu_3O_7$ specimen at 4·2 K, it is seen to satisfy the inequality $2H_I > H_{II}(0)$. In analogy with the results on semi-infinite geometries (Chaddah *et al* 1989b), we may now consider the linear relationship between the magnetic hysteresis and critical current density to be valid between H_I of 3 kOe and $(H_{max} - 5\,\text{kOe})$ at 4·2 K in the given $YBa_2Cu_3O_7$ powder.

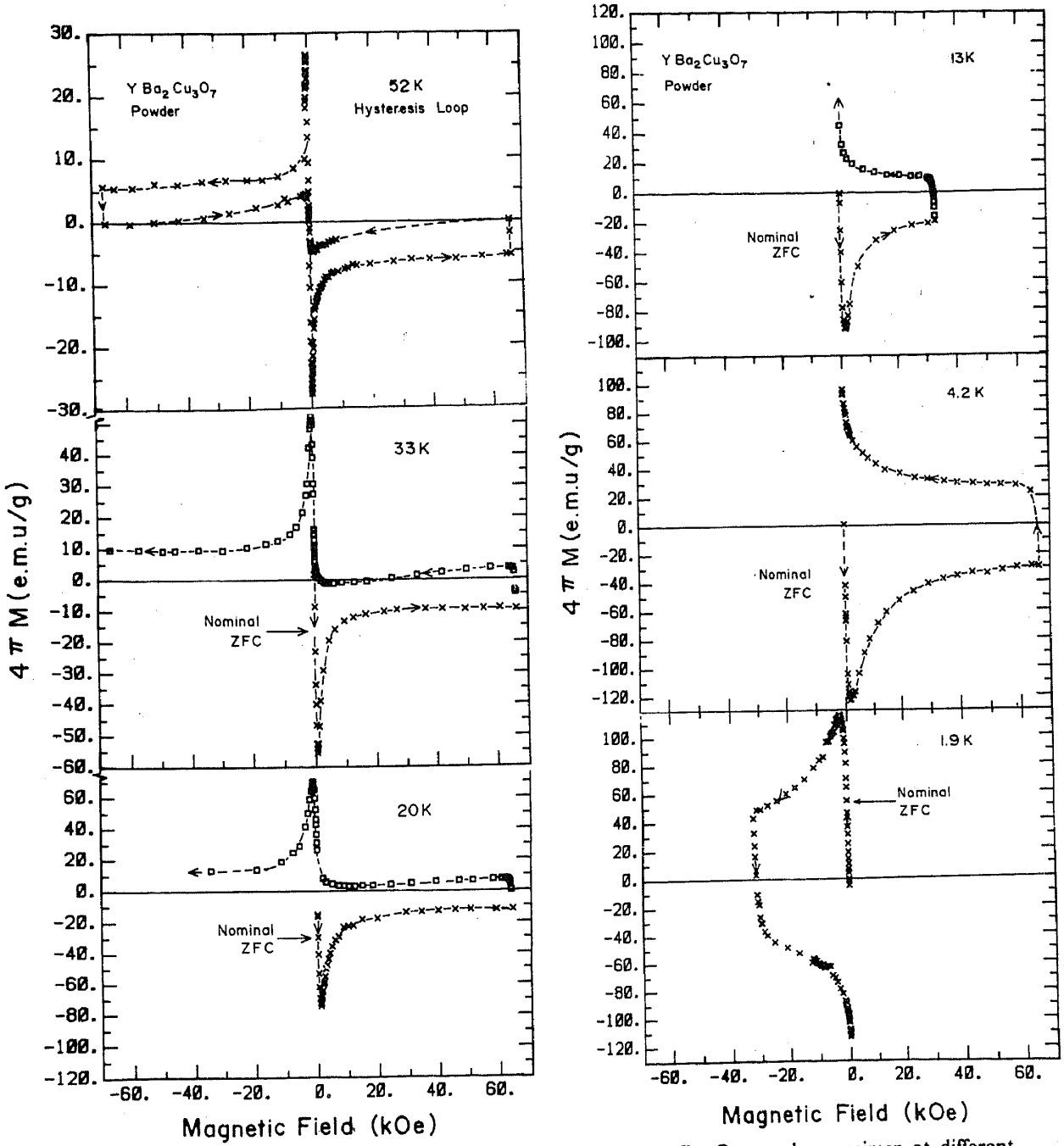

Figure 4. Magnetization hysteresis curves in $YBa_2Cu_3O_7$ powder specimen at different temperatures. The sample was cooled down to a given temperature in nominal zero field before ramping the field up and down. The nominal ZFC portion of the curve at 52 K has been omitted for clarity. At 1·9 K, the field was inadvertently ramped first in the negative direction after cooling in nominal zero field.

Figure 4 shows the magnetization hysteresis data in $YBa_2Cu_3O_7$ powder at different temperatures. These data were obtained using Faraday method. The complete hysteresis loop has been depicted for 52 K, whereas for other temperatures only the partial traces are shown. In particular, for 1·9, 4·2 and 13 K, the data have been plotted for the virgin run and the reverse hysteresis cycle down only to the zero field value. The reason for this incomplete presentation of the data would become apparent in §4 where the data for the subsequent part of the hysteresis cycle have also been presented. It may also be mentioned here that at 1·9 K, the field got inadvertently ramped first in the negative direction during the virgin run. Figure 5 shows the details of the hysteresis loop in Nb powder at 2·1 K. The merger point of nominal ZFC and forward hysteresis curves identifies $H_I(= 1{\cdot}4\,\text{kOe})$ values at 2·1 K, this is larger than the corresponding value at 4·2 K (cf. figure 2).

The data in figures 2, 5 and 6 can now be used to extract information about the field and temperature dependence of critical current density, averaged over arbitrary-shaped, randomly oriented particles with a certain size distribution. Before we do so, another point may be noted. For instance, the hysteresis loop in Nb at 2·1 K retains

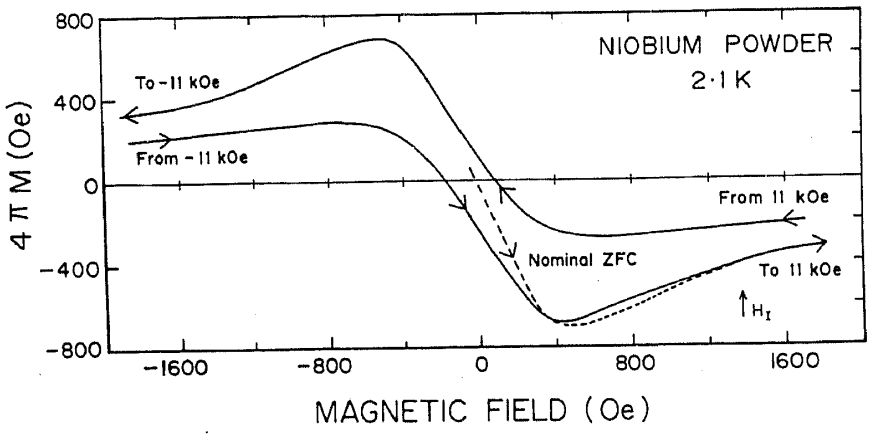

Figure 5. Magnetization hysteresis curve in niobium powder specimen at 2·1 K. The field value at which nominal ZFC and forward hysteresis curves merge identifies the H_1 value at 2·1 K in this specimen.

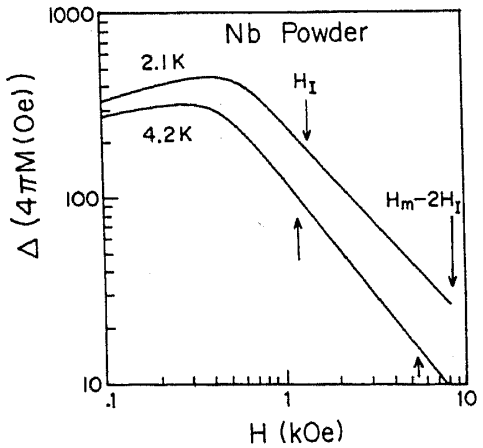

Figure 6. Log–log plot of $4\pi((M_\downarrow) - M(\uparrow))$ vs H in niobium powder specimen at 2·1 K and 4·2 K respectively. The arrows mark the H_I and $(H_{max} - 2H_I)$ values in each case. H_{max} is taken to be the H_{c2} value at a given temperature.

the shape it had at 4·2 K (cf. figures 2 and 5). However, in $YBa_2Cu_3O_7$, the shape of the hysteresis curve starts to undergo a qualitative change above 10 K. The hysteresis loop at 52 K is confined to the second and fourth quadrants, somewhat like the curves in Nb powder. This kind of transformation in the shape of hysteresis curves of $YBa_2Cu_3O_7$ is reported to occur in single crystal specimens (as a function of temperature (Senoussi *et al* 1988)) as well as in partially melted or Quench Melt Grown (QMG) specimens (as a consequence of crushing or heat treatment (Hein *et al* 1989 and Murakami *et al* 1989)). Trusting that the linear relationship between the width of the hysteresis and $J_c(H)$ would hold over a limited field region irrespective of the shape of the hysteresis loop, we show in figures 6 and 7 the plots of $\Delta M(H)$ (difference in magnetization values at a given H during the reverse and forward hysteresis paths) vs H in Nb powder and $YBa_2Cu_3O_7$ powder specimens respectively. The arrows in figure 6 define the interval, $H_1 < H < (H_m - 2H_1)$ at respective temperatures.

The proportionality constant $K(\equiv \Delta M(H)/J_c(H))$ depends on the sample shape, size, orientation etc. The particles constituting the powder specimen may have irregular shapes with a spread in size distribution, and they would also be randomly oriented vis-a-vis field direction. We have not attempted to estimate even the average values of K for the specimens under consideration. It suffices here to dwell qualitatively on some features of the field and temperature dependence of $\Delta M(H)$ in them. From the plots in figure 6, we may conclude that $\Delta M(H)$ ((or $J_c(H)$) decays as H^{-n} (where $n \simeq 1{\cdot}1$ to $1{\cdot}2$) in Nb powder at $T \leqslant 4{\cdot}2$ K. It is also apparent from figure 6 that the experimental $\Delta M(O)$ values at 4·2 K and 2·1 K are less than the $\Delta M(O)$ values that may be obtained from extrapolation of power law behaviour to $H = 0$ value. This feature is consistent with the claim made by Chaddah *et al* (1989b) on the basis of an argument presented for $J_c(H)$ decaying with H in semi-infinite geometries. The plots in figure 7 show that in $YBa_2Cu_3O_7$ powder, $\Delta M(H)$ would also fit to H^{-n} ($n \simeq 0{\cdot}3$ to $0{\cdot}4$) behaviour at $T \leqslant 13$ K, whereas at higher temperatures ($T \geqslant 20$ K) an anomalous kind of response is seen. For $T \geqslant 20$ K, $\Delta M(H)$ first decays with H followed by an up turn, and the field value corresponding to minimum in $\Delta M(H)$ decreases as T increases. This kind of behaviour has been noted by others also in polycrystalline

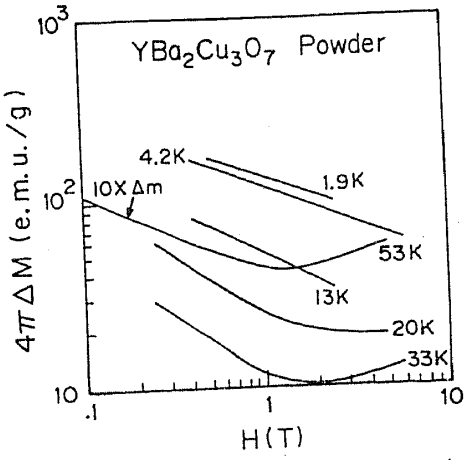

Figure 7. Log–log plot of $4\pi(M(\downarrow) - M(\uparrow))$ vs H in $YBa_2Cu_3O_7$ powder sample at different temperatures. The data at 52 K have been multiplied by 10 for convenience of presentation along with the data at other temperatures.

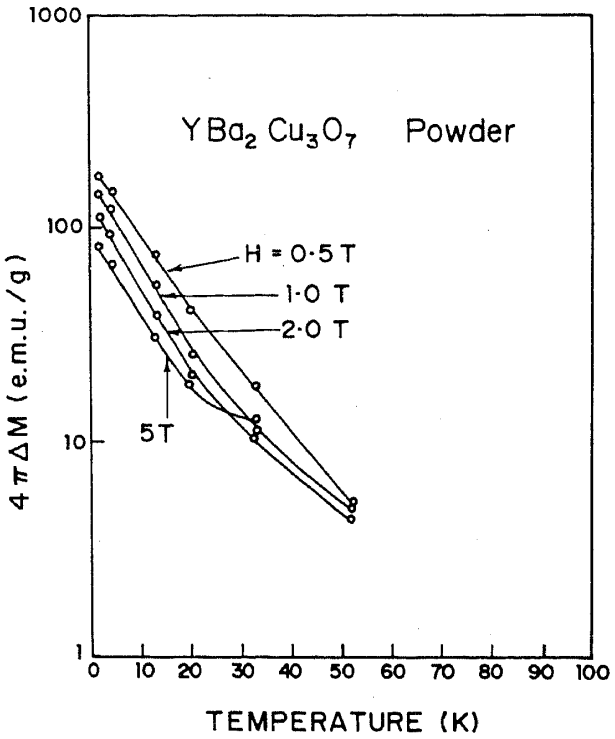

Figure 8. Semi-log plot of $4\pi(M(\downarrow) - M(\uparrow))$ vs temperature at field values of 0·5, 1·0 and 2·0 T respectively in $YBa_2Cu_3O_7$ powder.

as well as in single crystal specimens of $RBa_2Cu_3O_7$ family. It is speculated by some workers (Xu *et al* 1989 and Larbalestier *et al* 1990) that these materials are inhomogeneous and may be considered as comprising of two phases interwoven at atomistic level (e.g., oxygen-rich and oxygen-deficient regions) with one phase (oxygen-deficient) having lower H_{c2} than the other. Application of high enough magnetic field quanches superconductivity in lower H_{c2} regions which may then act as additional pinning centers for the remaining matrix. Another set of workers (Miu *et al* 1990) has argued that in superconducting specimens which can be considered as superposition of two components, a minimum in the field dependence of $J_c(H)$ can arise from demagnetizing effects associated with one component in the presence of pinning behaviour. As per their argument, the field value corresponding to the minimum in $J_c(H)$ should qualitatively correlate with the field value at which the zero field cooled magnetization curve peaks. The data in figures 4 and 7 do not seem to support contention of Miu *et al* 1990.

Figure 8 shows the plots of $\Delta M(H)$ vs T at a few H values in $YBa_2Cu_3O_7$ powder. For $H \leqslant 1$ T, $\Delta M(H)$ values appear to fit an exponential form over a limited temperature region ($T/T_c < 0{\cdot}5$) with decay constant, $T_0 \simeq 12 \pm 2$ K. On the basis of the data presented, we may therefore state that in the given $YBa_2Cu_3O_7$ powder specimen, $J_c(H, T) \alpha H^{-n} \exp(-T/T_0)$ for $T < T_c/2$, where $n \simeq 0{\cdot}3$ to $0{\cdot}4$ and $T_0 \simeq 12 \pm 2$ K.

3.2 *Thermomagnetic history effects*

Figures 9 to 11 show the magnetization curves in Nb rod, Nb powder and $YBa_2Cu_3O_7$ powder specimens obtained under various thermomagnetic histories at a few selected

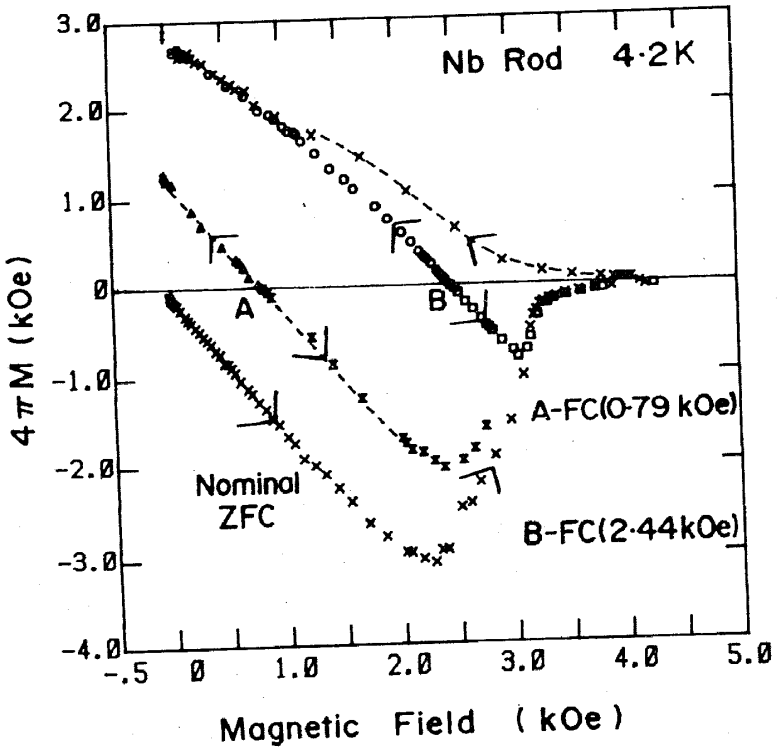

Figure 9. Magnetization curves in niobium rod ($l = 5$ mm, dia $= 1{\cdot}3$ mm) specimen obtained at 4·2 K under different thermomagnetic histories. For each of these runs, the sample was cooled down from above its T_c to 4·2 K in nominal zero field, 0·79 kOe and 2·44 kOe respectively. The arrows indicate the direction in which the field was varied after initial field cooling the sample. The points A and B on the magnetization axis mark the measured magnetization values on field cooling the specimen in fields of 0·79 and 2·44 kOe respectively. The nominal ZFC magnetization curve sketches out an envelope within which the rest of the magnetization curves are constrained to lie.

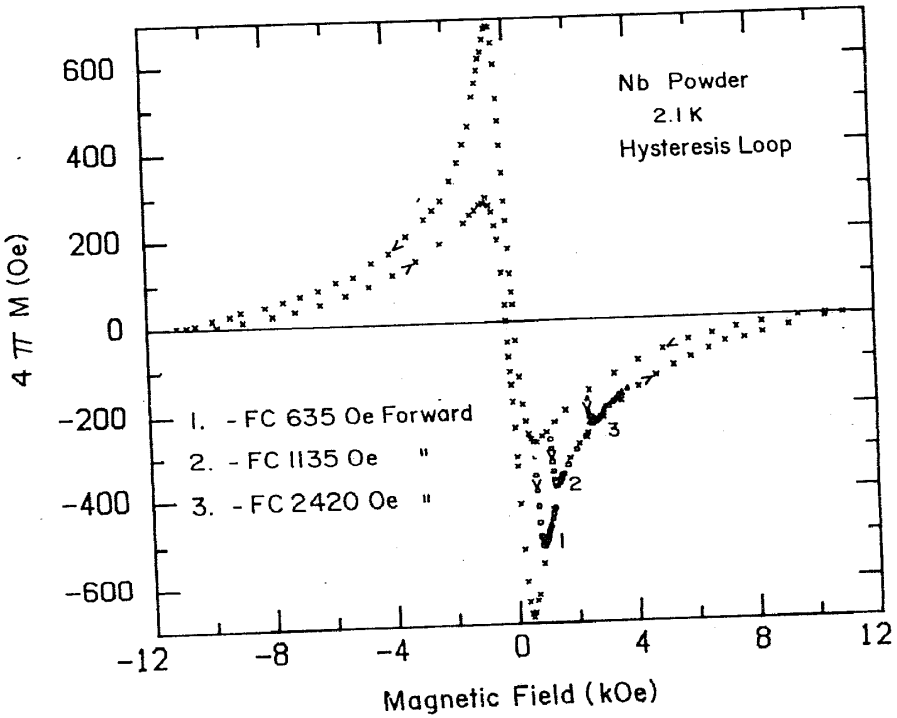

Figure 10a. Magnetization hysteresis curves in niobium powder specimen at 2·1 K obtained under different thermomagnetic histories. For the curves marked 1, 2 and 3, the sample was cooled down from above its T_c down to 2·1 K in fields of 635, 1135 and 2420 Oe respectively. In each of these cases, the field was then ramped up to 11 kOe. The data points denoted by crosses sketch out the complete hysteresis loop which forms an envelope within which the magnetization curves obtained with different thermomagnetic histories lie.

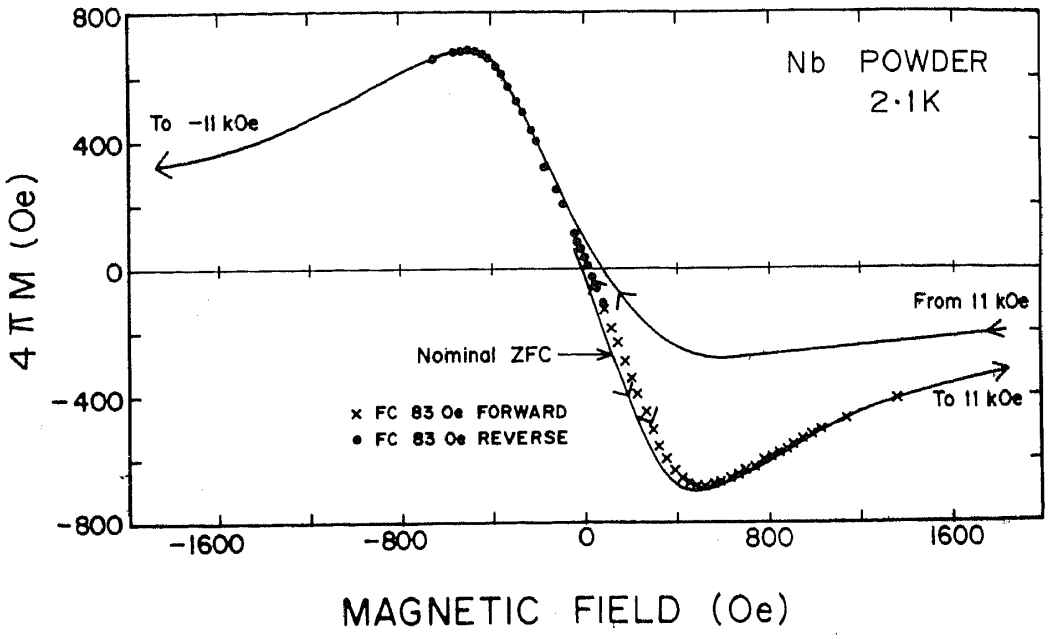

Figure 10b. The details of the forward and reverse magnetization curves in niobium powder specimen after cooling the sample down to 2·1 K in a field of 83 Oe.

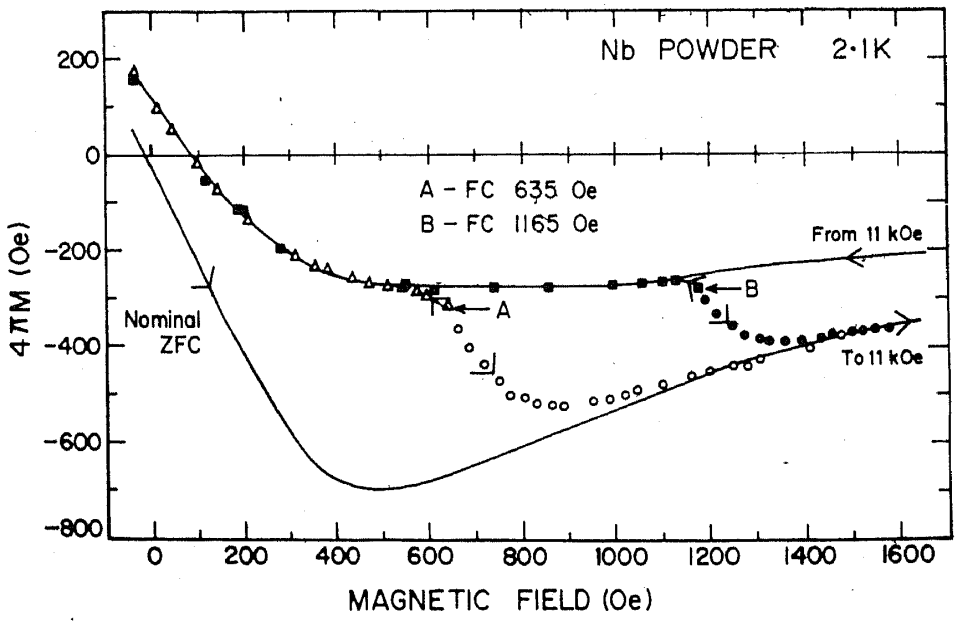

Figure 10c. The details of the forward and reverse magnetization curves in niobium powder specimen after field cooling to 2·1 K in 635 Oe and 1165 Oe respectively. The continuous lines sketch out the magnetization curve obtained after cooling the sample in nominal zero field. The data points A and B mark the field cooled magnetization values in 635 and 1165 Oe respectively. It may be noted that both A and B lie below the continuous line corresponding to the reverse path of the magnetization hysteresis loop. The reverse magnetization curves made up of open triangles and closed squares, initiating from data points A and B respectively, merge into the reverse hysteresis path.

temperatures in the region $T \leqslant 4{\cdot}2\,K$, using the Faraday method. The results of another study of thermomagnetic history effects at $T \geqslant 5\,K$ in a Nb rod of different shape and size and a Nb powder specimen using a different magnetometer have been presented earlier (Grover *et al* 1989). The new results on Nb and $YBa_2Cu_3O_7$ being presented together here essentially echo the inferences drawn from an analysis of data in Nb specimens by Grover *et al* 1989.

Figure 9 shows the forward and reverse magnetization curves in Nb rod sample after cooling the sample down to 4·2 K in 0·79 kOe and 2·44 kOe respectively. In this specimen, the field cooled magnetization (M_{FC}) values are observed to be almost zero, i.e., no flux spontaneously escapes the specimen as it undergoes superconducting transition in presence of applied field. $M_{FC}(H)$ curve in it therefore coincides with the applied magnetic field axis and this Nb rod specimen exemplifies the behaviour of a perfect conductor for any isothermal field variation in a field cooled (FC(H)) state. For instance, when the field is reduced or increased at points A or B in figure 9, the initial slope value is the same as that for a nominal ZFC sample indicating that the sample tends to perfectly shield the trapped flux from any external field change. The forward magnetization curves initiating from FC(H) states eventually merge with the nominal ZFC curve. The reverse magnetization curve for FC (2·44 kOe) state merges with the reverse hysteresis part of the nominal ZFC curve at positive field value

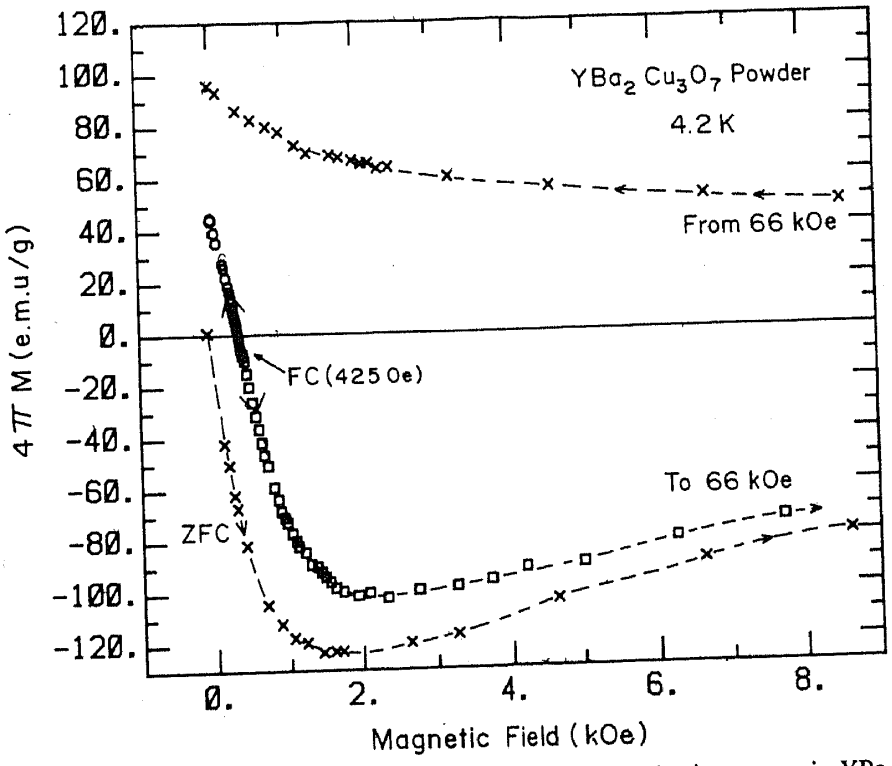

Figure 11a. The details of the forward and reverse magnetization curves in $YBa_2Cu_3O_7$ powder specimen after cooling the specimen down to 4·2 K in a field of 425 Oe. The arrow FC(425 Oe) marks the field cooled magnetization value at 4·2 K. The dotted line through cross data points sketches out the magnetization curve obtained after cooling the sample down to 4·2 K in nominal zero field. The FC(425 Oe) forward curve would merge into the nominal ZFC curve. The slope of FC(425 Oe) reverse curve is less than the slope of nominal ZFC forward curve in the field interval 425 to 0 Oe. Thus, $(M_{rem} - M_{FC}) < (-M_{ZFC})$ at $H = 425$ Oe.

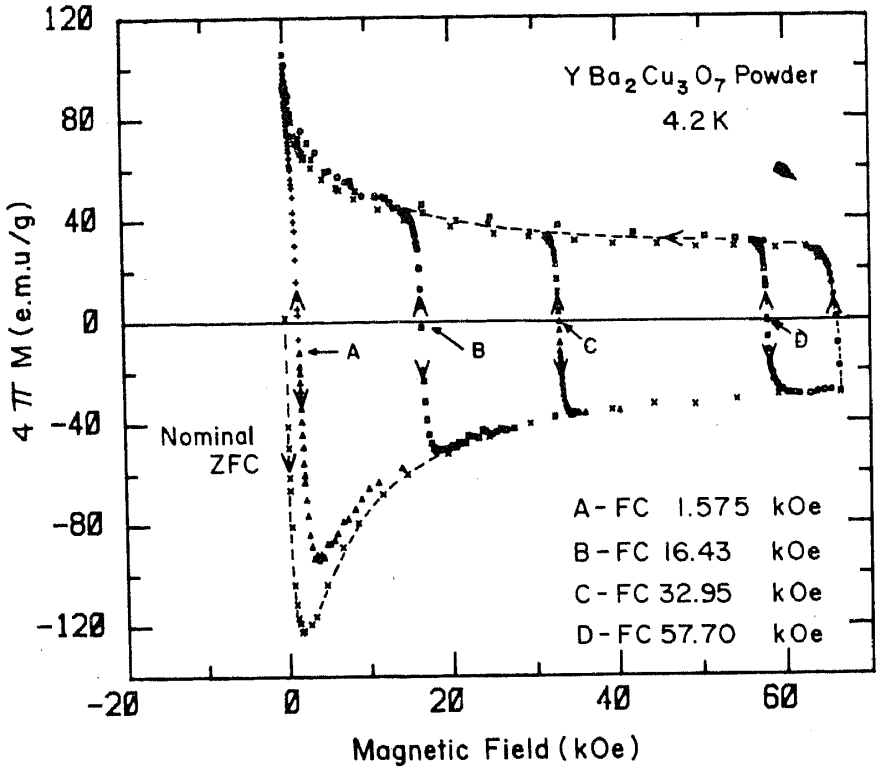

Figure 11b. The forward and reverse magnetization curves in $YBa_2Cu_3O_7$ powder specimen after field cooling to 4·2 K at the field values indicated. The data points A to D mark the field cooled magnetization values ($M_{FC}(H)$) at $H = 1{\cdot}575$, 16·43, 32·95 and 57·70 kOe respectively.

whereas the reverse magnetization curve for FC(0·79 kOe) state does not do so till $H = 0$ value. The interesection of a reverse magnetization curve with magnetization axis ($H = 0$ line) gives the remanent magnetization, M_{rem}, for a given FC(H) state. This remanent magnetization is to be distinguished from the remanent magnetization introduced in §3·1.

From figure 9, it is apparent that if the reverse magnetization curve for a FC(H) state is parallel to the ZFC curve over the field interval from H to O, then $M_{rem}(H)$ would equal $(-M_{ZFC}(H))$. It may be noted that $M_{rem}(0{\cdot}79\,kOe)$ is only slightly less than $(-M_{ZFC}(0{\cdot}79\,kOe))$, whereas $M_{rem}(2{\cdot}44\,kOe)$ is greater than $(-M_{ZFC}(2{\cdot}44\,kOe))$. Considering that $M_{FC}(H) = 0$ in this specimen, we may divide the entire field span of the hysteresis loop into three regions, where $(M_{rem} - M_{FC})$ is either equal to or less than or greater than $(-M_{ZFC})$.

Figures 10a to c show the forward and reverse magnetization curves in Nb powder sample after cooling the sample down to 2·1 K in 83, 635, 1165 and 2420 Oe respectively. Figures 11a and b show similar data in $YBa_2Cu_3O_7$ powder specimen at 4·2 K. In both these cases, $M_{FC}(H)$ values are non-zero and the specimens do not show complete trapping of magnetic flux on field cooling. However, the features alluded to in the description of the data in Nb rod sample are evident in figures 10 and 11 as well. In addition, there are a few other interesting details in figures 10 and 11. All the important facts may be summarized as follows:

(i) The initial slope value of a forward or reverse magnetization curve for any FC(H) state is the same as that of its ZFC curves. This confirms that the specimens tend to shield the trapped flux from any change in externally applied field.

(ii) The forward and reverse FC(H) curves merge with the ZFC magnetization curve. This implies that the complete hysteresis loop comprising of forward and reverse hysteresis paths defines the envelope within which all the magnetization curves obtained under different thermomagnetic histories are constrained to lie. The field value at which the merger of the forward (or reverse) magnetization curve of a given FC(H) state occurs depends on the initial H value. The field interval between the initial H value and the field value at which the magnetization curve along the forward (or reverse) path merges into the magnetization curve along the forward (or reverse) hysteresis path decreases as H increases. The two intervals corresponding to the merger along the forward or the reverse paths for a given FC(H) state are not equal. It may be noted amongst the reverse curves that the merger occurs at negative fields for low H value (see, for instance, figure 10b), whereas it occurs at positive fields for higher values of H. It may be kept on view that the upper limit on the field interval between initial H value (in which the sample is field cooled) and the field value at which the forward curve meets the magnetization curve along forward hysteresis path is limiting field value H_1.

(iii) The reverse magnetization curve of a FC(H) sample is linear down to zero value for small H values (cf. figures 10b and 10c and figures 11a and 11b). In Nb powder sample at $H = 83$ Oe (figure 10b), the slope value of reverse curve is nearly equal to the corresponding value for the nominal ZFC curve. Such a behaviour implies the relationship $M_{rem}(H) - M_{FC}(H) = -M_{ZFC}(H)$. However, in $YBa_2Cu_3O_7$ powder at $H = 425$ Oe, the slope value of the reverse magnetization curve between 425 Oe and 0 Oe is smaller than its value for the ZFC curve in the same interval (see figure 11a), thus $M_{rem}(H) - M_{FC}(H) < -M_{ZFC}(H)$ at $H = 425$ Oe in this specimen. The equality relationship in $YBa_2Cu_3O_7$ powder would hold at much lower field values at 4·2 K, as has been reported by Shaw *et al* (1990). The reverse magnetization curves become progressively more non-linear as H increases further (see figures 10c and 11b). The $M_{rem}(H)$ values saturate beyond a limiting H value for which the reverse FC(H) curve starts to merge with the reverse hysteresis path at a positive field value. It is apparent from the data in figures 10 and 11 that after the M_{ZFC} curve turns over, the difference $(M_{FC}(H) - M_{ZFC}(H))$ progressively decreases as H increases. The saturated value of M_{rem} at some stage (see figure 11b) would exceed the difference $(M_{FC}(H) - M_{ZFC}(H))$, since this difference is expected to asymptotically vanish as $H \to H_{c2}$. Thus we can identify three field regions in these data, corresponding to $(M_{rem}(H) - M_{FC}(H) + M_{ZFC}(H)$ being equal to, less than or greater than zero.

Malozemoff *et al* (1988) were the first to focus attention onto the equality relationship, $M_{rem}(H) = M_{FC}(H) - M_{ZFC}(H)$, on the basis of their data recorded at 4·2 K and up to 160 Oe in powder and single crystal specimens of $YBa_2Cu_3O_7$. From the arguments presented by them, it can be seen that this equality relationship holds under the following two conditions: (i) the field H is less than the lower critical field H_{c1} at the given temperature, and (ii) no flux escapes from the field cooled state of the sample as the field is reduced to zero. The latter condition amounts to stating that the response of the sample during field removal is dictated only by the infinite conductivity property of the sample, which as mentioned earlier is the basic premise of Bean's critical state model. In the framework of this model, for $J_c(H)$ decaying with field, it has been shown earlier (Grover *et al* 1989) by drawing schematic field profiles for sample geometry of an infinite slab that the equality of Malozemoff *et al* (1988) is replaced by the inequality, $M_{rem}(H) < (M_{FC}(H) - M_{ZFC}(H))$ for $H > H_{c1}$ and

at very high H values, the inequality changes sign such that, $M_{rem}(H) > (M_{FC}(H) - M_{ZFC}(H))$. Most of the other features summarized above also qualitatively conform to the deductions made on the basis of schematics worked out by Grover *et al* (1989) for an inifinite slab in the limit that (i) $H_{c1} = 0$ and (ii) all flux is trapped on field cooling. One noteworthy exception is that the above mentioned schematics demands that the reverse magnetization for a FC(H) sample should merge with the reverse path of the loop only for $H > H_1$. In niobium powder at 2·1 K, the reverse magnetization curve for FC(635 Oe) merges with the reverse hysteresis (see figure 10c) at positive field even though $H_1 = 1400$ Oe (see figure 5). This inconsistency, we believe, is due to simplifying assumptions of complete irreversibility and $H_{c1} = 0$, both of which are not tenable in Nb powder.

It is of interest here to recall the irreversible behaviour observed (Shoenberg 1952; Andrew and Lock 1950; DeSorbo and Healy 1964; Heubner 1979; Grover *et al* 1990, 1991a) in cylindrical specimens of type-I superconductors when the field is applied parallel to the cylindrical axis. The irreversibility of the intermediate state of a type-I superconductor is a consequence of surface edge effects and the thermomagnetic history dependent non-uniform domain structure (DeSorbo and Healy 1964; Heubner 1979). The non-uniformity of the domain structure in a type I superconductor is very different from the non-uniform magnetic state of a hard type-II superconductor in its critical state. The major part of the remanent magnetization observed in type I superconductors is considered to be associated with a persistent current set up on a closed loop of a right angle (w.r.t. the applied field direction) edge (Shoenberg 1952; DeSorbo and Healy 1964). We anticipate that it would be possible to identify three field regions in the hysteresis loop of a type I superconductor, where $(M_{rem}(H) + M_{FC}(H) - M_{ZFC}(H))$ is either $=$, or $<$, or > 0. It may also be mentioned here that the inhomogeneities of the intermediate and the critical state of type I and hard type II superconductors respectively result (Ravi Kumar *et al* 1990; Grover *et al* 1991b) in contributions from multipole moments higher than the dipole moment of the specimens to the measured magnetization signal. Although the intermediate and mixed states of two types of superconductors manifest themselves in a similar way in their bulk magnetization response, their underlying physical basis are different.

4. Anomalous variations in magnetization

It is well-known (Bean 1962, 1964) that in hard superconductors the field value at which the magnetic flux penetrates a zero field cooled sample, to an experimentally measurable extent, gets dictated not only by its lower critical field H_{c1} but also by its size and J_c value. Thus, it is known that in high temperature superconducting materials which have large intragrain J_c values, the criterion of deviation from linearity of a zero field cooled magnetization curve may give gross overestimate of H_{c1} values in them (Ravi Kumar and Chaddah 1989a, b). This artifact has recently been vividly demonstrated by Martinez *et al* (1990) by quantitative analysis of zero field magnetization curve in a single crystal of $YBa_2Cu_4O_8$. On the basis of a model calculation, Ravi Kumar and Chaddah (1988, 1989b) had also proposed that H_{c1} can instead manifest as an anomalous variation around $H = 0$ line in the hysteritic part of the magnetization curve. Anomalous variations near $H = 0$ line in magnetic hysteresis curves of a few high temperature superconducting specimens have been

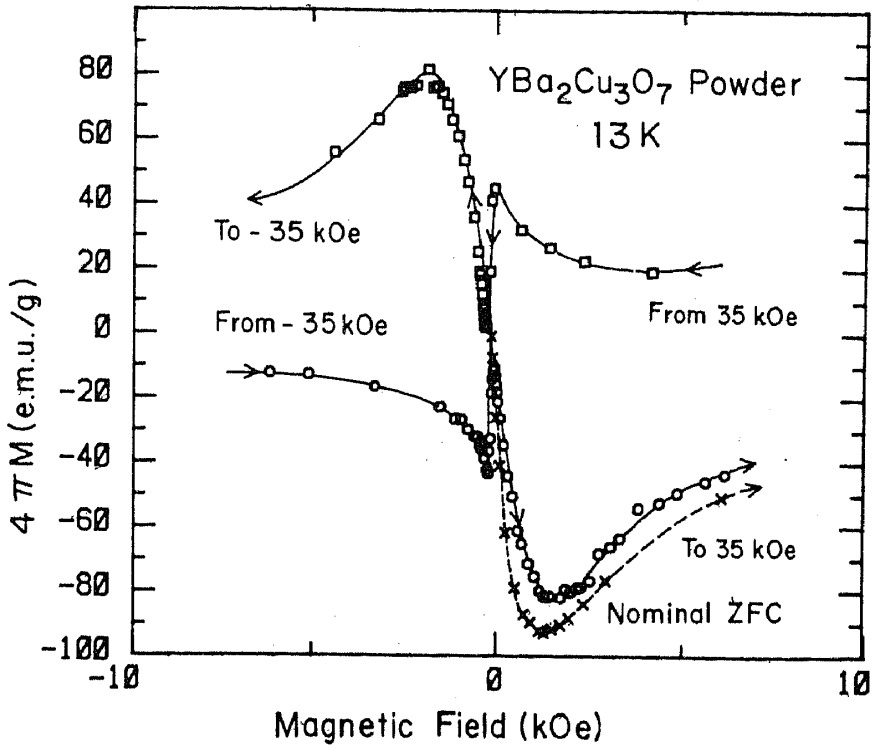

Figure 12a. The details of the forward and reverse magnetization hysteresis curves across the region of nominal zero field in $YBa_2Cu_3O_7$ powder specimen at 13 K. The arrows indicate the way the magnetization changes anomalously across the region of zero field. The initial portion of the nominal ZFC curve is also shown by dotted line for comparison.

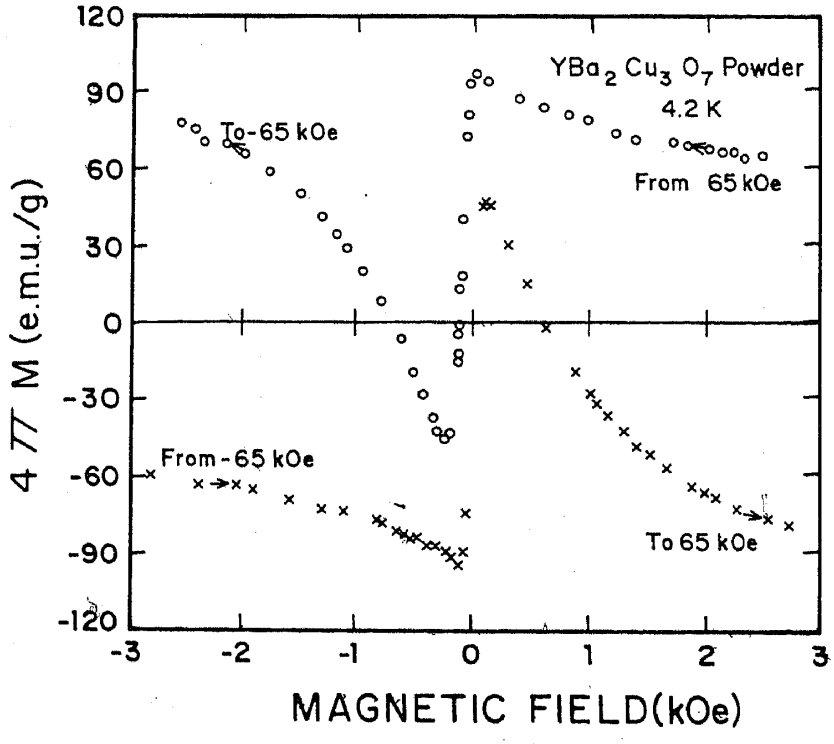

Figure 12b. The details of the forward and reverse magnetization hysteresis curves across the region of zero field in $YBa_2Cu_3O_7$ powder specimen at 4·2 K.

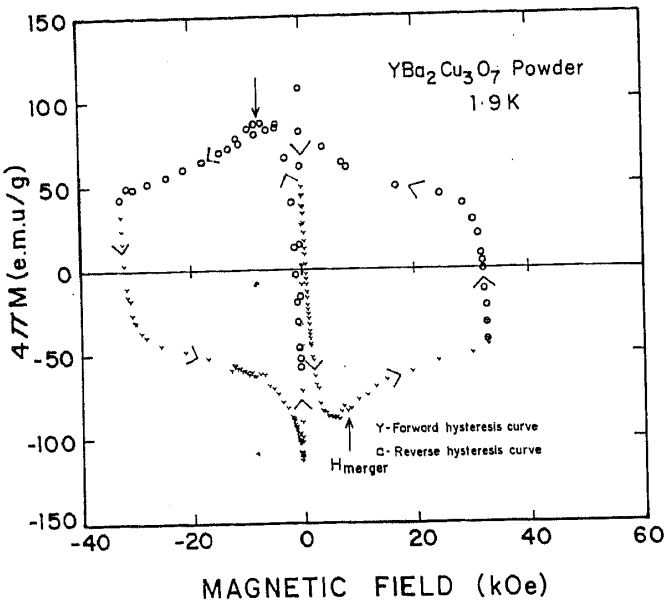

Figure 13. The complete hysteresis loop in $YBa_2Cu_3O_7$ powder sample obtained at 1·9 K on repeated cycling of the field between ± 35 kOe. The arrows mark the way magnetization changes on variation of field. The anomalous variations in magnetization on moving across the zero field region can be clearly identified. The H_{merger} identifies the field value at which the nominal ZFC curve at 1·9 K of figure 4 would merge into the curve along the hysteresis path ($\pm H_{max}$ to $\mp H_{max}$).

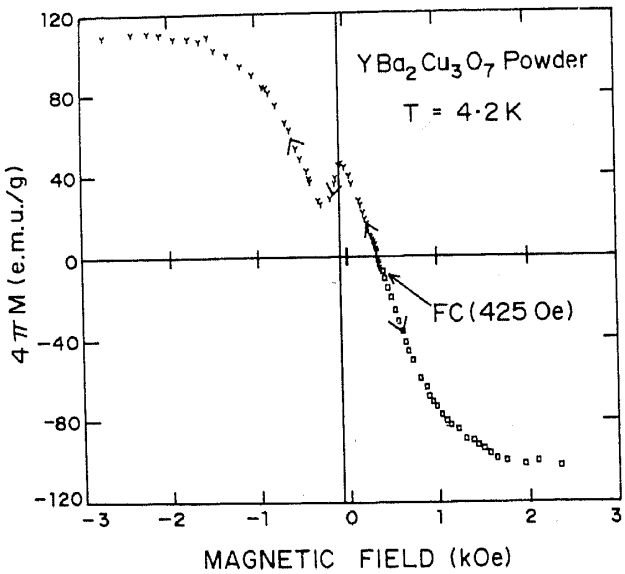

Figure 14. Details of the forward and reverse magnetization curves in $YBa_2Cu_3O_7$ powder specimen at 4·2 K on cooling the specimen in a field of 425 Oe. An anomalous dip in magnetization values across the nominal zero field value in the reverse curve can be noted.

reported in the literature (Grover *et al* 1988; Chaddah *et al* 1989a; Schneemeyer *et al* 1987; Grader *et al* 1988; van-Dover *et al* 1988) and if these are identified with the model calculations of Ravi Kumar and Chaddah (1988, 1989b), they would imply a H_{c1} of a few Oe in these materials. To further clarify the situation regarding these observed anomalous variations across $H = 0$ region, we carefully reinvestigated some

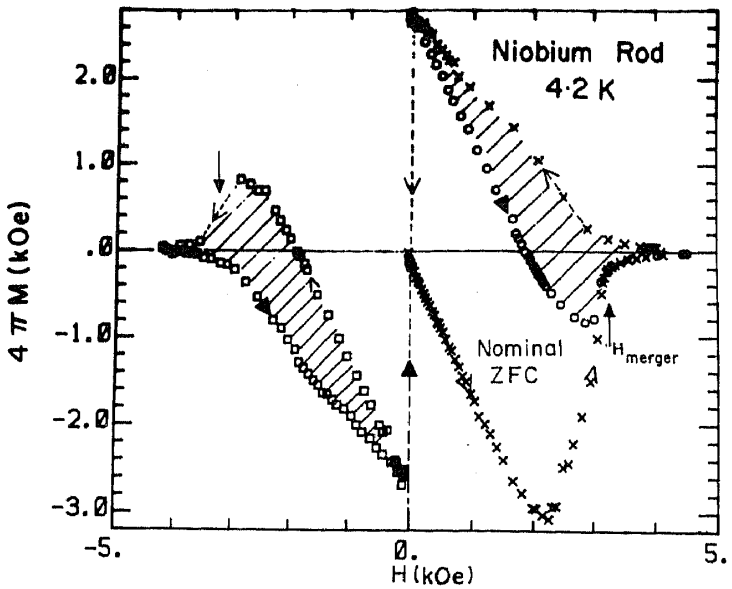

Figure 15. The magnetization hysteresis curve in niobium rod specimen at 4·2 K. The arrows mark the way magnetization changes on variation of field across the region of nominal zero field. The field value H_{merger} marks the limiting field at which the nominal ZFC curve and the forward hysteresis curves overlap. The remanent magnetization almost completely reverses on moving across the zero field region. Due to this, the hysteresis loop of niobium rod specimen at 4·2 K comprises of just two lobes identified by the hatched region. The nominal ZFC curve appears to remain outside the domain of this hysteresis loop.

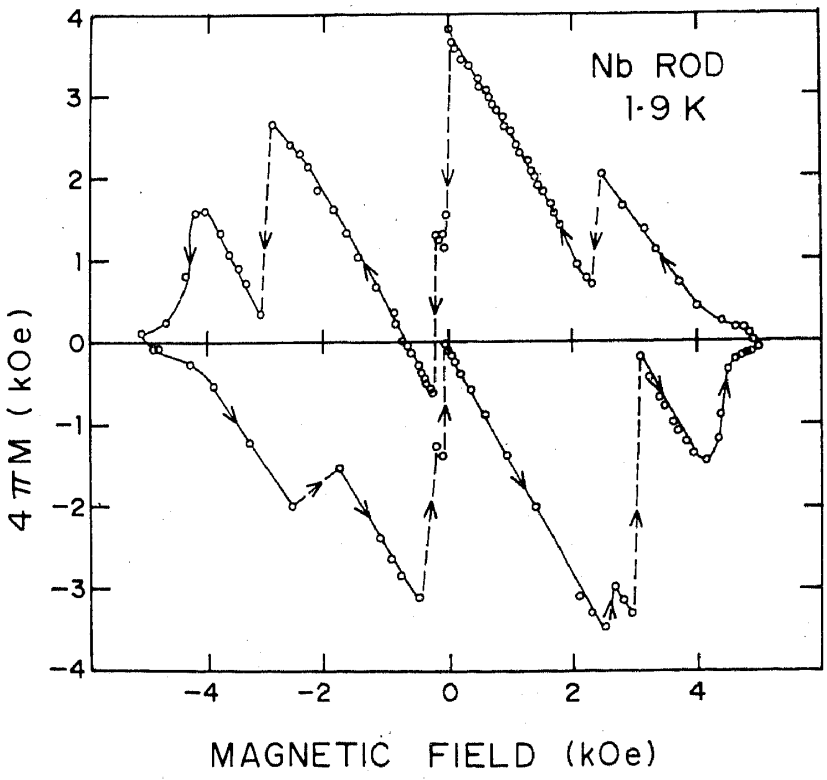

Figure 16. The magnetization hysteresis data in niobium rod specimen at 1·9 K. The dotted lines indicate the flux jumps.

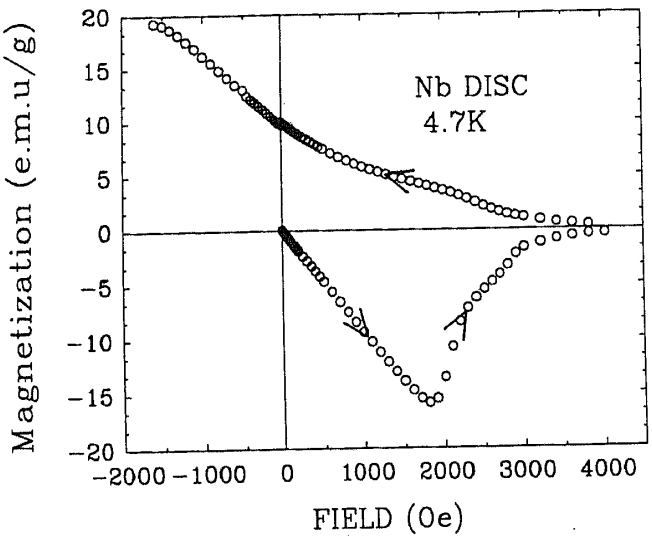

Figure 17. Magnetization hysteresis curve at 4·7 K in a thin disc niobium specimen for field applied parallel to the plane of the disc. The data have been obtained using SQUID magnetometer. No anomalous variation in magnetization is observed on moving across the region of zero field.

of them in $YBa_2Cu_3O_7$ powder and the niobium rod samples using two different magnetometers. Figures 12 to 17 summarize the data obtained. Figures 12 to 14 show anomalous variations in magnetization values on going across the region of nominal zero field in $YBa_2Cu_3O_7$ powder sample. Figures 15 and 16 show the anomalous variations as well as the phenomenon of magnetic flux jumps in niobium specimen in the shape of rod with field applied perpendicular to the cylindrical axis. Figure 17 shows the absence of any anomalous behaviour in the magnetization hysteresis response in Nb specimen in the shape of a thin disc with field applied parallel to the plane of the disc.

In figures 1 and 2 we had shown the complete hysteresis loops in Nb and $YBa_2Cu_3O_7$ powders obtained at 4·2 K using the Faraday method and the SQUID magnetometer respectively. There is no anomalous looking feature across the $H = 0$ line in these two magnetization hysteresis curves. However, in $YBa_2Cu_3O_7$ powder, when the data are obtained using the Faraday method, anomalous variations are observed across $H = 0$ line below a certain temperature. Figures 12a and b show the details of the magnetization curves along different paths across the nominal zero field (residual field of the superconducting magnet) line at 13 K and 4·2 K respectively in $YBa_2Cu_3O_7$ powder. It may be noted that on going across the region of nominal zero field along the reverse hysteresis path, the magnetization first decreases and then increases as the steady field produced by the superconducting magnet is ramped in the negative direction. A similar anomalous variation (almost a mirror image) in magnetization values is visible on going across the nominal zero field line during the forward hysteresis run. That this type of anomalous behaviour is temperature dependent is apparent from the fact that such a response was not observed in the data recorded on the same sample at $T \geqslant 20$ K (see reverse hysteresis curves for $T \geqslant 20$ K across the nominal zero field line in figure 4). The vertical height of this anomalous dip in magnetization values measured from the remanent magnetization value, is seen to increase as temperature decreases (see reverse and forward hysteresis curves at 4·2 K and 1·9 K in figures 12b and 13 respectively).

Figure 15 shows the magnetization data at 4·2 K in Nb rod sample obtained using the Faraday method. In these data one notices that the remanent magnetization completely reverses sign on moving across the nominal zero field line. The vertical height of the anomalous dip (or rise) in magnetization values in this case is therefore equal to twice the remanent magnetization. After the remanent magnetization has reversed, as the applied field is increased further, the magnetization curve obtained possesses the same topological characteristics as evident from its nominal ZFC curve. For instance, the difference between the reversed remanent magnetization value and the peak magnetization value during the reverse hysteresis path is almost equal to the peak magnetization value of the nominal ZFC curve (see figure 15). It is also interesting to note that the two lobes identified by hatched regions in figure 15 constitute the hysteresis loop in Nb rod sample at 4·2 K. The field value H_{merger} in figure 15 marks the limiting field at which the nominal ZFC and the forward hysteresis curves overlap. This field in figure 15 is not the same as the limiting field H_1 introduced earlier because of the phenomenon of reversal of remanent magnetization. However, the connotation that at $H > H_{\text{merger}}$ in figure 15, the memory of the previous magnetic history is lost appears to remain valid. The hysteresis loop for $YBa_2Cu_3O_7$ specimen at 1·9 K depicted in figure 13 is the topological equivalent of the two lobes of figure 15. The initial part of the ZFC magnetization curve at 1·9 K (as depicted in figure 4) would remain outside the hysteresis loop of figure 13 which also appears to comprise of two split bubbles equivalent to the two lobes of figure 15. An apparent difference in the shapes of two hysteresis loops in figures 13 and 15 is a consequence of the difference in their H_{merger} values relative to the total field regions over which the hysteresis loops span. The field value at which the nominal ZFC curve of $YBa_2Cu_3O_7$ powder at 1·9 K (shown in figure 4) merges with the hysteresis curve is indicated by H_{merger} in figure 13. The anomalous variations pertaining to the reversal of remanant magnetization remain confined to a narrow central region of the hysteresis loop in figure 13 (in contrast to a much larger span in figure 15) and these features in figure 13 are likely to be overlooked in those experimental runs where data are recorded at coarse intervals. It may be noted here that the above kind of anomalous behaviour can also be mentioned in the data on a $YBa_2Cu_3O_7$ specimen reported by Fuller *et al* (1987) (see their figure 1).

Figure 14 shows the magnetization curves obtained along increasing and decreasing field directions after having cooled the $YBa_2Cu_3O_7$ powder specimen down to 4·2 K in a field of 425 Oe. An anomalous dip in magnetization values on going across the region of nominal zero field along the direction of decreasing field can be clearly seen in the data of figure 14. It was noted (all the data not being shown here) that the vertical height of this anomalous dip at 4·2 K gradually decreased as the remanent magnetization decreased. The smallness of the dip in figure 14 amounts to a tiny decrease of the remanent magnetization in contrast to near complete reversal of the remanent magnetization evident in the figure 13. However, the field interval over which the magnetization first decreases before picking up again is roughly the same (about 200 Oe) in figures 13 and 14. But, in Nb rod, the field interval over which the remanence reversed completely was observed to be much smaller (about 10 Oe). We believe that the absence of observation of anomalous variation in the data of Nb powder (see figures 1 and 5) is due to smallness of remanent magnetization in this specimen.

We have no definite clue as to what triggers the reorientation of the remanent magnetization across the region of zero field in the data obtained with Faraday

method. We did not observe any anomalous variation during the magnetization measurements on the same $YBa_2Cu_3O_7$ powder specimen using a SQUID magnetometer (cf. figures 2 and 12b). Figure 17 shows the magnetization data at 4·7 K in a thin disc-shaped specimen of Nb (machined out of the same 6 mm diameter rod) for field applied parallel to the plane of the disc obtained using the SQUID magnetometer. There is no anomalous variation evident on going across the zero field region along the reverse hysteresis path in these data as well. However, anomalous variations are present in the data on a $YBa_2Cu_3O_7$ specimen obtained using a SQUID magnetometer by Fuller *et al* (1987). The anomalous variations described above do not appear to be a part of the well documented phenomenon of flux jumps occurring at field values spread all over the total field span as can be easily identified (see dotted lines) in the data of figure 16. These flux jumps are present even when the experiment is repeated on a SQUID magnetometer.

In view of the above, it is possible that some of the anomalous variations visible in figures 12 to 15 are an artifact of the experimental conditions under which the magnetization curves are obtained. We are therefore not inclined to identify these variations with the model calculations of Ravi Kumar and Chaddah (1988, 1989b) to estimate H_{c1} values in the given speciments. It may be recalled here that the physical basis of their model is that the flux spontaneously escapes from the surface regions of the specimen as the local field becomes less than H_{c1} on going across the region of zero field. This contention of theirs does not seem to find support from the reverse magnetization curve for FC (0·79 kOe) state at 4·2 K in Nb rod sample (see figure 9) whose H_{c1} value is estimated to be about 1 kOe. The situation relating to the model of Ravi Kumar and Chaddah (1988) for $YBa_2Cu_3O_7$ and other high temperature superconducting compounds is not clear at present as a true consensus on the estimates of H_{c1} values in them is yet to emerge. For instance, the estimated values for $H_{c1}(\perp c)$ in different compounds range from a few Oe to $\sim 10^2$ Oe (see Chaddah 1991).

5. Temporal effects

The magnetization of a hard superconductor has long been known to decay with time at finite temperatures. Müller *et al* (1987) were the first to focus attention onto the time decay of magnetization in a high temperature copper oxide superconductor. They found that in a ceramic specimen La–Ba–Cu–O, M_{ZFC}, M_{FC} and M_{rem} decay differently. An understanding of the time decay of magnetization in conventional superconductors was initiated by Anderson (1962) based on the phenomenon of thermal activation of flux bundles over an effective pining potential in the direction of the flux gradient. This has since been theoretically investigated by many people, the critical state model and its various extensions have been combined with Anderson's flux creep idea and several predictions (Chaddah and Ravi Kumar 1989c) made regarding the field and temperature dependences of decay rates of magnetic states having different thermomagnetic histories. In particular, on the basis of calculations performed for infinite geometries ($N = 0$), Chaddah and Ravi Kumar (1989b) have pointed out certain topological features (see, in particular, their figure 3) that may exist in behaviour of time decay of magnetization in hard superconductors. For instance it has been stated (Chaddah and Ravi Kumar 1989b) that, (i) the decay rate of magnetization with field-on (M_{ZFC}) is expected to be more than that of the magnetization with field-off (the remanent magnetization M_R of § 3.1) for small H

values, (ii) the field-on decay rate is expected to reach its maximum value at $H = H_I$ and (iii) the decay rate for field-off will become independent of field for $H > H_{II}(O)$.

We have looked for some of the above mentioned topological features in powder specimens of $YBa_2Cu_3O_7$ and compared them with the data deduced from the results of an experiment on a specimen of a conventional hard superconductor V_3Si (Fraser *et al* 1989). Our measurements have been made using a quantum design SQUID magnetometer and a Faraday balance susceptometer (George Associates Inc. Model nos 300 & 320 with an electromagnet). In a routine mode of operation, the quantum design SQUID magnetometer does not provide data about magnetization decay during the initial 50–100 sec, whereas in the other Farday susceptometer, reliable data about magnetization decay can be obtained after the initial 500 m sec. We

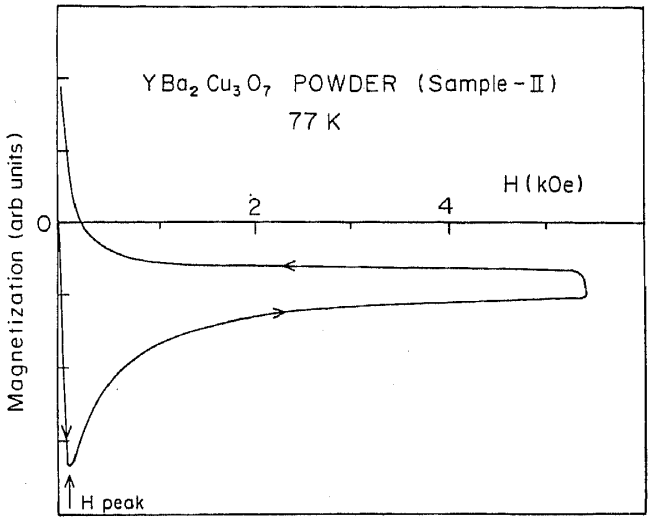

Figure 18. Magnetization hysteresis curve in $YBa_2Cu_3O_7$ powder (sample-II) at 77 K. The H_{peak} identifies the field value ($\simeq$ 125 Oe) at which the virgin magnetization peaks at 77 K in this specimen.

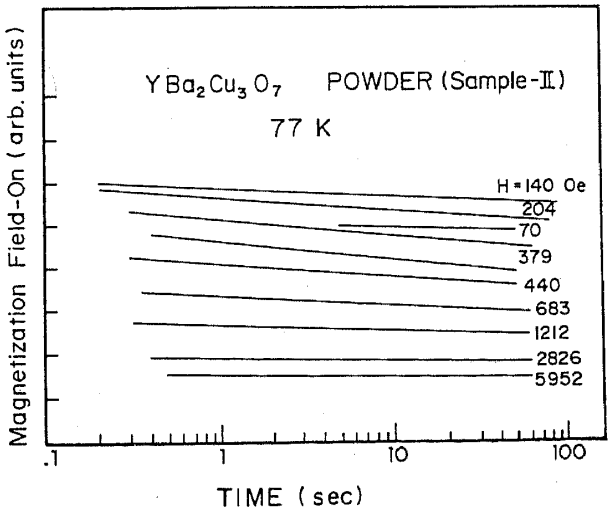

Figure 19. Semi-log plot of field-on magnetization (M_{ZFC}) with time at different field values in $YBa_2Cu_3O_7$ powder (sample-II) at 77 K. The zero magnetization value for each of the curves in this figure is located at different place, i.e., the curves are arbitrarily placed as regards the vertical axis. However, the y-scale has been kept the same for all the curves to give an idea of relative values of $\Delta M/\Delta(\log t)$ at different field values which are plotted in figure 20.

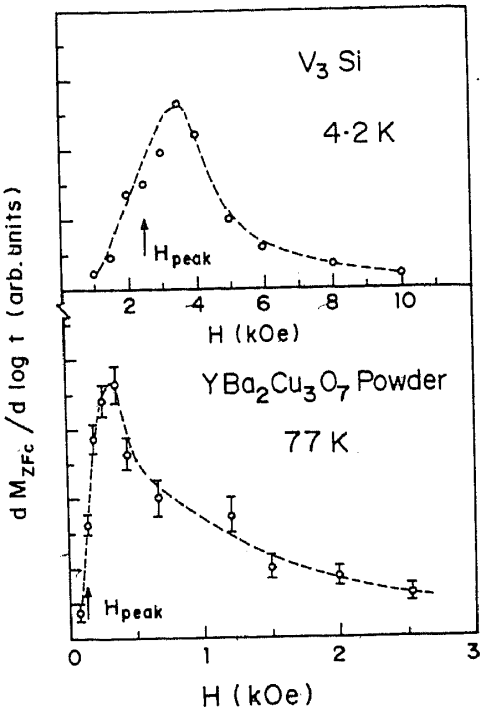

Figure 20. Plots of $dM_{ZFC}/d\log t$ vs H in a V_3Si specimen at 4·2 K and in $YBa_2Cu_3O_7$ powder (sample-II) at 77 K. The arrows mark the H_{peak} values in the respective specimens. The field values at which $dM_{ZFC}/d\log t$ curves peak identify the H_I values in respective specimens at respective temperatures.

employed the quantum design SQUID magnetometer to record the time dependence of field-on and field-off magnetizations at different field values at 5 K. The time decay of field-on magnetization at 77 K was recorded using the Faraday susceptometer. In the Faraday susceptometer the field-gradient (of 6 Oe/cm) was kept-on all through the record of the time evolution of magnetization values. It was ensured that there was no drift in the microbalance output in the chosen range of operation in the field-gradient off situation. Figures 18 to 22 summarize most of the data obtained.

The $YBa_2Cu_3O_7$ powder specimen used for time decay measurements is different from the one used earlier for magnetization hysteresis and thermomagnetic history effect studies. In this second specimen (to be referred to as $YBa_2Cu_3O_7$ sample-II), the virgin magnetization M_{ZFC} at 5 K peaks at about 3 kOe instead of at 1·7 kOe (see, for instance, figure 4) as in the first $YBa_2Cu_3O_7$ specimen.

Figure 18 shows the magnetization hysteresis curve at 77 K in $YBa_2Cu_3O_7$ powder sample-II, the $H_{peak}(= 125$ Oe) denotes the field value at which the virgin magnetization peaks. Figure 19 shows the field-on magnetization (M_{ZFC}) vs time at 77 K at various field values. From such data, one can ascertain the values of $dM_{ZFC}/d\ln t$ for different H. Figure 20 shows the plots of $dM_{ZFC}/d\ln t$ vs H in $YBa_2Cu_3O_7$ powder at 77 K and V_3Si sample at 4·2 K. The values for V_3Si have been deduced from magnetization vs time data of Fraser *et al* (1989). The data for V_3Si had been obtained in the similar time window (1–50 sec) as ours. In figure 20, it can be noted that $dM_{ZFC}/d\ln t$ curves peak at field values higher than the corresponding H_{peak} values in specimens of a high temperature superconductor and a conventional superconductor. The field value corresponding to the peak position of $dM_{ZFC}/d\ln t$ may be taken as an estimate of H_I value of the given specimen at a given temperature.

Figure 21 shows the plots of field-on magnetization ($4\pi M_{ZFC}$) vs $\ln t$ in $YBa_2Cu_3O_7$

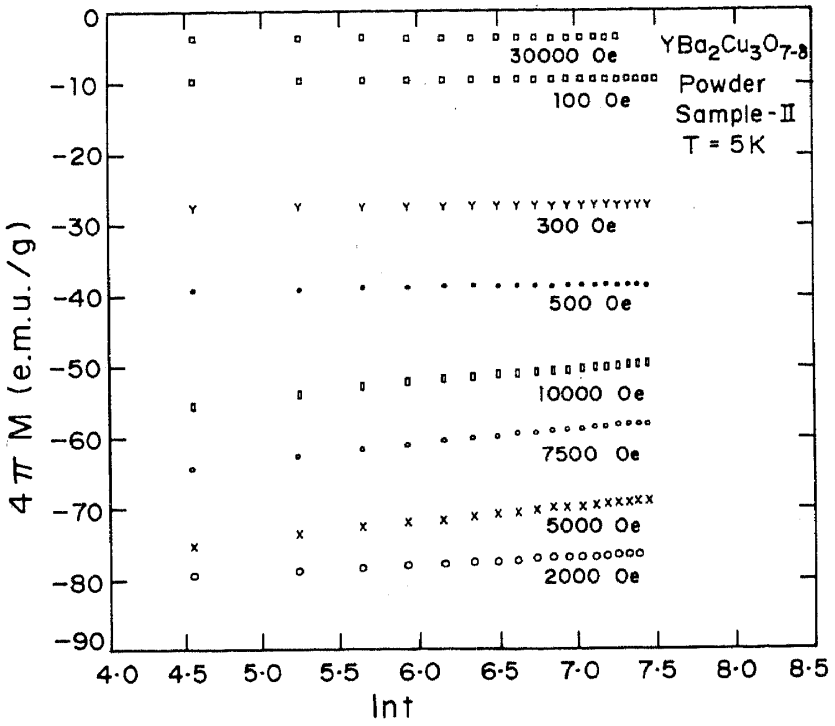

Figure 21. Variation of field-on magnetization (M_{ZFC}) vs ln t at 5 K in $YBa_2Cu_3O_7$ powder (sample-II) at different field values.

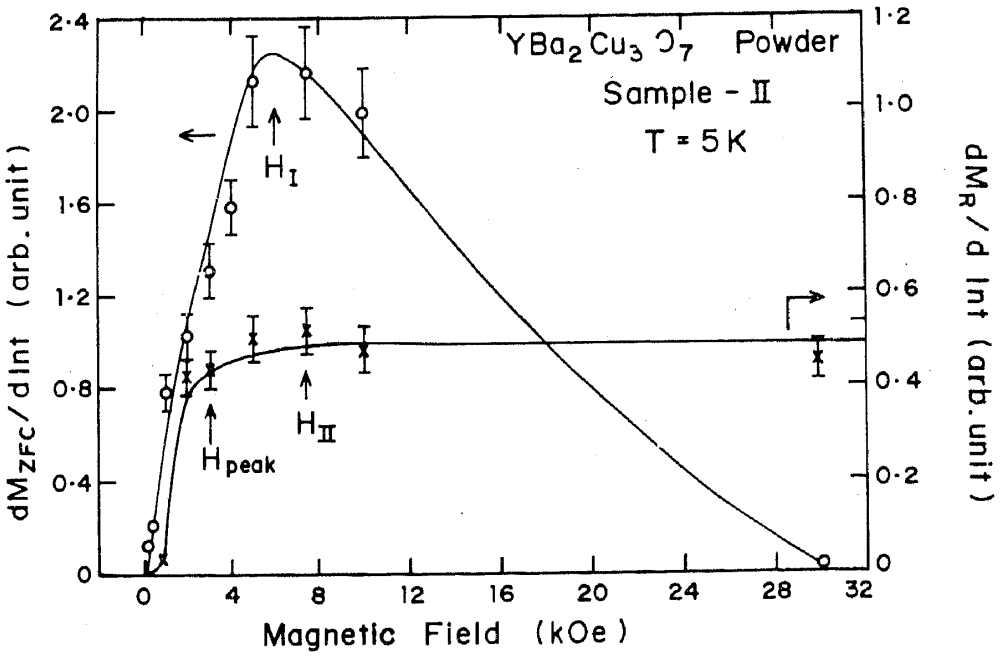

Figure 22. Variation of $dM_{ZFC}/d\ln t$ and $dM_R/d\ln t$ vs H at 5 K in $YBa_2Cu_3O_7$ powder (sample-II). The H_{peak}, H_I and $H_{II}(O)$ values in this specimen at 5 K are also indicated.

powder sample-II at 5 K at different field values. Similar data for field-off magnetization values (M_R) have not been shown for brevity. Figure 22 shows the plots of deduced values of $dM_{ZFC}/d\ln t$ and $dM_R/d\ln t$ vs H at 5K. The values of H_{peak} (= 3 kOe), H_I(= 5 kOe) and $H_{II}(O)$(= 8 kOe) 5 K in $YBa_2Cu_3O_7$ powder specimen-II have also been indicated in figure 22. The values may be compared with the H_{peak}, H_I and H_{II} values of 1·7 kOe, 3 kOe and 5 kOe respectively in $YBa_2Cu_3O_7$ powder sample-I, on

which detailed magnetization data had been recorded (cf. § 3). It may be mentioned here that Mota *et al* (1989) had earlier reported the field dependence of remanence magnetization M_R and the decay rate $dM_R/d\ln t$ in a specimen of a conventional hard superconductor $Pb_{0.6}In_{0.4}$ alloy. In that specimen also, M_R and $dM_R/d\ln t$ can be seen to show saturation at the same field value (i.e., the $H_{II}(O)$ value) as in the case of $YBa_2Cu_3O_7$ sample-II in figure 22.

6. Summary

To summarize, we have presented the results of experimental studies on magnetization in specimens of a conventional superconductor niobium and a high temperature superconductor $YBa_2Cu_3O_7$. We have presented a comparative study of hysteresis in magnetization, thermomagnetic history effects, anomalies in magnetic hysteresis response and the time decay of magnetization in specimens belonging to the families of conventional type-II and high temperature superconductors. The Bean's critical state model and its various possible extensions are considered adequate to explain many features in the magnetic behaviour of conventional hard superconductors. The similarity of the topological features observed in the results of various magnetization experiments conducted on specimens of the two families underscore the utility of the above model in understanding several aspects of the bulk magnetic response of high temperature superconductors as well.

Acknowledgements

One of us (BVBS) would like to put on record the hospitality of Solid State Physics Group of TIFR, Bombay during his visiting professorship there. We are grateful to Dr P Chaddah for sharing with us his insights into the magnetic response of hard superconductors. It is also a pleasure to acknowledge Prof. R Srinivasan for giving us an access to the SQUID magnetometer operational at IIT Madras. We thank Prof. G V Subbarao of Material Science Research Centre of IIT Madras for giving us good quality sintered samples ($T_c = 90$ K) of $YBa_2Cu_3O_7$.

References

Andrew E R and Lock J M 1950 *Proc. Phys. Soc.* (*London*) **A63** 13
Anderson P W 1962 *Phys. Rev. Lett.* **9** 309
Bean C P 1962 *Phys. Rev. Lett.* **8** 250
Bean C P 1964 *Rev. Mod. Phys.* **36** 31
Bhagwat K V and Chaddah P 1989 *Pramana – J. Phys.* **33** 521
Bhagwat K V and Chaddah P 1990 *Physica* **C166** 1
Bhagwat K V and Chaddah P 1991 *Phys. Rev.* **B** (submitted)
Chaddah P, Ravi Kumar G, Grover A K, Radhakrishnamurty C and Subbarao G V 1989a *Cryogenics* **29** 907
Chaddah P, Bhagwat K V and Ravi Kumar G 1989b *Physica* **C159** 570
Chaddah P and Ravi Kumar G 1989c *Phase transitions* **19** 37
Chaddah P 1991 *Pramana – J. Phys.* **36** 353
Chen D X and Glodfarb R B 1989 *J. Appl. Phys.* **66** 2510
Chen D X, Sanchez A and Munoz J S 1990a *J. Appl. Phys.* **67** 3430

Chen D X, Sanchez A, Nogues J and Munoz J S 1990b *Phys. Rev.* **B41** 9510
DeSorbo W and Healy W A 1964 *Cryogenics* **4** 257
DeSorbo W 1963 *Phys. Rev.* **123** 107
DeSorbo W 1964 *Phys. Rev.* **A134** 1119
Deutscher G and Müller K A 1987 *Phys. Rev. Lett.* **59** 1745
Fietz W A and Webb W W 1969 *Phys. Rev.* **178** 657
Finnemore D K, Stromberg T F and Swenson C A 1966 *Phys. Rev.* **149** 231
Fraser J R, Finlayson T R and Smith T F 1989 *Physica* **C 159** 70
Fuller W W, Osofsky M S, Toth L E, Qadri S B, Lawrence S H, Hein R A, Gubser D U, Francavilla T L and Wolf S A 1987 *Jpn. J. Appl. Phys. Suppl.* **26–3** 1189
Grader G S, Gyorgy E M, Gallagher P K, O'Bryan H M, Johnson Jr. D W, Sunshine S, Jim S and Sherwood R C 1988 *Phys. Rev.* **38** 757
Grover A K, Radhakrishnamurty C, Chaddah P, Ravi Kumar G and Subbarao G V 1988 *Pramana – J. Phys.* **30** 569
Grover A K, Paulose P L, Chaddah P and Ravi Kumar G 1989 *Pramana – J. Phys.* **33** 297
Grover A K, Ravi Kumar, Chaddah P, Subramanian C K and Sankaranarayanan V 1990 *Physica* **C170** 431
Grover A K, Ravi Kumar, Malik S K, Chaddah P, Sankaranarayanan V and Subramanian C K 1991a *Phys. Rev.* **B43** 6151
Grover A K, Ravi Kumar, Malik S K and Chaddah P 1991b *Solid State Commun.* **77** 723
Grover A K and Chaddah P 1991 in *Some theoretical and experimental aspects of superconductivity*, (ed) L C Gupta (New York: Nova Science Publishers Inc.) (in press)
Hein R A, Hojaji H, Barkatt A, Shafii H, Michael K A, Thorpe A N, Ware M F and Alterescu S 1989 *J. Superconduct.* **2** 427
Heubener R P 1979 *Magnetic flux structures in superconductors, Springer Series in Solid State Sciences*, Vol. 6 ch. 2
Larbalestier D C and Daeumling M 1990 preprint; Daeumling M, Seuntijens J M and Larbalestier D C 1990 *Nature – London* **346** 332
Malozemoff A P, Krusin-Elbaum L, Cronemeyer D C, Yeshurun Y and Holtzberg F 1988 *Phys. Rev.* **B38** 6490
Malozemoff A P 1989 in *Physical properties of high temperature superconductors* (ed.) D M Ginsberg (Singapore: World Scientific), pp 71–150 and references therein
Malozemoff A P, Krusin-Elbaum L and Clem J R 1989 *Physica* **C162–164** 353
Martin S, Fiory A T, Fleming R M, Espinosa G P and Cooper A S 1989 *Appl. Phys. Lett.* **54** 72
Martinez J C, Prejan J J, Karpinski J, Kaldis E and Bordet P 1990 *Solid State Commun.* **75** 315
Miu L, Gn. Aldica, Horobiowski M and Wlosewicz D 1990 *On the valley-effect in the magnetic field dependence of the critical current density in high-T_c superconducting ceramics*, preprint
Mota A C, Juri G, Visani P and Pollini A 1989 *Physica* **C162–164** 1152
Müller K A, Takashige M and Bednorz J G 1987 *Phys. Rev. Lett.* **58** 1143
Murakami M, Morita M and Koyama N 1989 *Jpn. J. Appl. Phys.* **28** L1125
Ravi Kumar G and Chaddah P 1988 *Pramana – J. Phys.* **31** 505
Ravi Kumar G and Chaddah P 1989a *Phys. Rev.* **B39** 4704
Ravi Kumar G and Chaddah P 1989b *J. Superconduct.* **2** 247
Ravi Kumar, Grover A K, Chaddah P, Subramanian C K and Sankaranarayanan V 1990 *Solid State Commun.* **76** 175
Sarkissian B V B, Grover A K, Balakrishnan G, Paulose P L and Vijayaraghavan R 1989 *Physica* **C162–164** 335
Schneemeyer L F, Gyorgy E M and Waszczak J V 1987 *Phys. Rev.* **B36** 8804
Senoussi S, Oussena M, Collin G and Campbell I A 1988 *Phys. Rev.* **B37** 9792
Shaw G, Bhagat S M, Spencer N D, Crow J E and Tyagi S 1990 *Physica* **C169** 257
Shoenberg D 1952 *Superconductivity* (New York, Cambridge: University Press) p 34
van-Dover R B, Schneemeyer L F, Gyorgy E M and Waszczak J V 1988 *Appl. Phys. Lett.* **52** 1910
Yun-Hui Xu, Wei-Yan Guan, Ziebig K and Heiden C 1989 *Cryogenics* **29** 281